Flame-ion probe of the reaction zone in a CH_4–O_2–Ar flame with added HCN, NH_3 and NO

JOHN M. GOODINGS, GARY B. DE BROU,[1] AND DIETHARD K. BOHME

Department of Chemistry, York University, 4700 Keele Street, Downsview, Ont., Canada M3J 1P3

Received October 22, 1980

This paper was presented at a Special Symposium "The Structure and Thermochemistry of Gaseous Ions," held in honour of Dr. F. P. Lossing of the National Research Council of Canada, during the Second Canadian Conference on the Gas Phase Chemistry of Ions, Trent University, June 5–8, 1980, and is dedicated to him on the occasion of his 65th birthday

JOHN M. GOODINGS, GARY B. DE BROU, and DIETHARD K. BOHME. Can. J. Chem. **59**, 1810 (1981).

The addition of 0.3% of the fuel-nitrogen (fuel-N) compounds HCN, NH_3, or NO to a premixed, fuel-rich, CH_4–O_2–Ar flame burning at atmospheric pressure demonstrated the rapid interconversion of nitrogenous intermediates in the reaction zone. The nitrogenous species (HCN/CN, HNCO/NCO, NH_3, NH_2, NH, NO, NO_2) were observed as ions (CN^-, H_2CN^+, NCO^-, H_2NCO^+, NH_4^+, NH_3^+, NH_2^+, NO^+, NO_2^-, and hydrate ions) formed in chemical ionization processes discussed previously (1). The ions were sampled directly into a flame-ion mass spectrometer which had sufficient spatial resolution for the measurement of ion concentration profiles through the reaction zone. The study bears on Fenimore's suggestion for the formation of "prompt NO" in fuel-rich hydrocarbon flames. These additive results were compared with previous results involving nitrogenous species present in a similar CH_4–O_2 flame doped with 10% N_2. The increased sensitivity of the additive approach confirmed many of the mass assignments and mechanisms involved in the N_2 study. Reasonably good evidence was obtained for the elusive intermediate HNCO (and possibly isomeric HCNO as well) in protonated form, and also formamide, NH_2CHO, which had not been detected previously. Similarities in profile peak positions and magnitudes observed for many ions, irrespective of the nature of the fuel-N additive, indicated that the nitrogenous species were linked by a network of fast bimolecular reactions, many of which appeared to be balanced in the reaction zone.

JOHN M. GOODINGS, GARY B. DE BROU et DIETHARD K. BOHME. Can. J. Chem. **59**, 1810 (1981).

L'addition de 0,3% de combustibles azotés (combustible-N) HCN, NH_3 ou NO à la flamme de CH_4–O_2–Ar riche en combustible, prémélangée et brûlant à pression atmosphérique démontre qu'il se produit une interconversion rapide des intermédiaires azotés dans la zone de réaction. On a observé que les espèces azotées (HCN/CN, HNCO/NCO, NH_3, NH_2, NH, NO, NO_2) sont présentes sous forme d'ions (CN^-, H_2CN^+, NCO^-, H_2NCO^+, NH_4^+, NH_3^+, HN_2^+, NO^+, NO_2^- et sous forme d'ions hydratés) formés selon un processus d'ionisation chimiques discuté antérieurement (1). Les échantillons d'ions sont injectés directement dans un spectromètre de masse à ionisation par flamme qui a une résolution spatiale suffisante pour mesurer les profils de concentrations en ions dans la zone de réaction. L'étude est reliée à la suggestion de Fenimore relative à la formation "rapide de NO" dans des flammes d'hydrocarbures riches en combustibles. On a comparé ces résultats additifs aux résultats antérieurs impliquant des espèces azotées présentes dans un flamme semblable de CH_4–O_2 dopée avec 10% de N_2. L'augmentation de la sensibilité dans l'approche additive confirme plusieurs des attributions de masse et des mécanismes impliqués dans l'étude du N_2. Les données obtenues sont suffisantes pour justifier la présence de l'intermédiaire insaisissable HNCO (et peut être aussi de son isomère HCNO) sous forme protonée ainsi que du formamide NH_2CHO, qui n'avait pas été décelé antérieurement. Des ressemblances dans les profils des positions des pics, dans les amplitudes observées pour plusieurs ions, indépendamment de la nature de l'additif combustible-N indiquent que les espèces azotées sont liées par un réseau de réactions bimoléculaires rapides dont plusieurs semblent être balancées dans la zone de réaction.

[Traduit par je journal]

Introduction

In a previous paper (1), we discussed how flame ionization can be employed as a probe for nitrogenous intermediates leading to NO_x formation in the reaction zone and burnt gas of CH_4–O_2–N_2 flames. Ion concentration profiles along the axis of a fuel-rich flame indicated the presence of nitrogenous ions (CN^-, H_2CN^+, NCO^-, NH_2^+, NH_3^+, NH_4^+, NO^+, NO_2^-) formed in chemical ionization (CI) processes of nitrogenous neutral species (CN/HCN, NCO/HNCO, NH, NH_2, NH_3, NO, NO_2). The relevant ion chemistry was discussed in detail. The nitrogenous neutral chemistry based on Fenimore's initial concept of "prompt NO" (2) in fuel-rich hydrocarbon combustion was briefly summarized, involving a sequence of nitrogenous intermediates N_2–HCN–HNCO–NH_i (i = 0–3)–NO_x; a recent and detailed review is available (3).

The experiments to be described here involve stepping into this sequence at various stages by the addition of 0.3% of fuel-nitrogen (fuel-N) in the form of HCN, NH_3, and NO to essentially the same methane–oxygen flame discussed previously (1). In similar experiments involving a variety of fuel-N additives, Morley (4) used a flame-ion mass spectrometer to sample the nitrogenous ions present in hydrocarbon flames. His published data pertain to the region downstream of the reaction zone in the

---

[1] Present address: Ministry of the Environment, Air Resources Branch, 880 Bay Street, Toronto, Ont., Canada M5S 1Z8.

0008-4042/81/121810-09$01.00/0

burnt gas. In our case, we emphasize nitrogenous ions present in the reaction zone of conical flames where the chemistry is initiated, taking advantage of good spatial resolution. Flame-ion sampling is one of a very few techniques available for probing the reaction zone of a flame and, while possibly causing some distortion of the ion concentrations, is unlikely to falsify the result in any qualitative sense.

The high concentrations of available nitrogen from the addition of HCN, NH_3, and NO clarify the identities of the nitrogenous species present in the reaction zone which were reported in our previous study of N_2-doped flames (1). The data also offer confirmation of the kinds of CI processes which are dominant. Perhaps most important, however, is the demonstration of the rapid interconversion of the nitrogenous neutral intermediates within the confines of the reaction zone, a distance ca. 0.3 mm corresponding to a residence time <300 μs.

Experimental

The results will be presented for five variations of essentially the same fuel-rich, premixed, CH_4–O_2-diluent flame burning at atmospheric pressure. The CH_4 and O_2 flow rates were always maintained at 8.00 and 7.90 mL s^{-1}, respectively, amounting to an equivalence ratio $\phi = 2.03$. Flame 1 had a diluent flow rate of Ar of 2.15 mL s^{-1}. Flame 2 had a diluent flow rate of N_2 of 1.69 mL s^{-1}, amounting to a molar dilution of the unburnt gas of roughly 10%. The Ar flow rate for flame 1 was chosen so that flames 1 and 2 had the same adiabatic flame temperature of 2510 ± 20 K. These are the two flames which have been described and studied previously (1). Flames 3, 4, and 5 are the same as flame 1 with the addition of 0.3 mol% of HCN, NH_3, and NO, respectively. Such a small amount of an additive is not expected to have any appreciable effect on the physical flame characteristics (5). The constancy of the measured sampling temperature was checked for flame 4 (NH_3 additive) and flame 1 using a pneumatic probe consisting of two critical-flow (i.e., choked-flow) orifices in series described previously (1, 6). The compressed gases used were all of CP grade (CH_4 > 99.6%, O_2 > 99.6%, N_2 > 99.9%, Ar > 99.9%). The HCN was added as a 2.7 ± 0.1% mixture of HCN in Ar. The NH_3 (anhydrous, >99.99%) and NO (CP grade, >99.0%) were added directly from lecture bottles into the premixed gas stream.

All flames were laminar with conical luminous reaction zones (height ~5 mm, base diameter ~3 mm, thickness ~0.3 mm) to facilitate ionic sampling along the flame axis into a mass spectrometer. The burnt gas velocity was approximately 1 m s^{-1}. The flames were stabilized on a simple, tubular, quartz burner (2.3 mm id) surrounded by a flowing argon shield to minimize the entrainment of atmospheric air. The burner was mounted on a motor-driven carriage with accurate axial alignment and calibrated drive providing spatial resolution of ±0.02 mm along the flame axis (designated z) for both positive and negative ion profiles.

The flame-ion mass spectrometer has been described previously in detail (7) and in summary form (1). For these additive studies, the flame burned against a 60°, conical, chromium, sampling nozzle of orifice diameter ca. 0.1 mm mounted in a water-cooled flange. The sampled ions pass through two stages of differential pumping into a quadrupole mass filter. The mass-analyzed ions are detected with a parallel-plate Faraday cage connected to a vibrating reed electrometer having a grid-leak resistance of 10^{11} ohms. The ion signal magnitudes in Figs. 2, 3, and 5 are quoted in mV based on the detected ion current passing through 10^{11} ohms. Profiles can be drawn for ion species having a peak concentration as low as 5×10^5 ions mL^{-1}, corresponding to a signal magnitude of about 0.5 mV. A method has been described (1, 7) for locating a reproducible origin ($z \equiv 0$) in the *flame* (not referred to the burner) corresponding to the downstream edge of the luminous reaction zone on the flame axis. In this way, a family of ion profiles at different mass numbers (m/e), can be accurately overlaid on the distance scale z.

Results and Discussion

Total Ion Profiles

In order to appreciate the behaviour of individual ion signals, it is first necessary to recognize the effects of the additives on the total ionization characteristics of the flames. Total ion profiles, both positive and negative, are shown in Fig. 1 for each of the five flames. The total positive profiles are shown normalized to unity at the profile maxima. This constancy of peak signal corresponding to approximately 10^{10} ion mL^{-1} was observed to be true within an experimental error of ±10%. It reflects the basic chemi-ionization process responsible for the formation of flame ions in the reaction zone (8, 9)

$$[1] \quad CH + O \rightarrow HCO^+ + e^-$$

whose rate will be approximately constant for all five flames at the same temperature. An appreciable upstream shoulder is apparent for flame 4 (NH_3 additive), and a smaller one for flame 5 (NO), but is absent in flames 3 (HCN) and 2 (N_2). These shoulders are indicative of an additional chemi-ionization source term. One such process deduced by other workers (10) to be responsible for the ions observed in an NH_3–O_2–N_2 flame

$$[2a] \quad N(2^2D) + O(^3P) \rightarrow NO^+ + e^-$$

might be applicable here, particularly if the order of availability for excited N atoms in the chemical decomposition of the nitrogen additives is NH_3 > NO > HCN, N_2. A second reaction which has been considered as a source of ions in CO–O_2–N_2 (11) or H_2 – air diffusion (12) flames, both with added cyanogen, C_2N_2

$$[2b] \quad CN + O + O \rightarrow NO^+ + e^- + CO$$

is less likely to be significant in the fuel-rich flames employed in this study; in any case, it is of little help in explaining the absence of a shoulder with the HCN additive (flame 3).

In contrast, a considerable enhancement of the

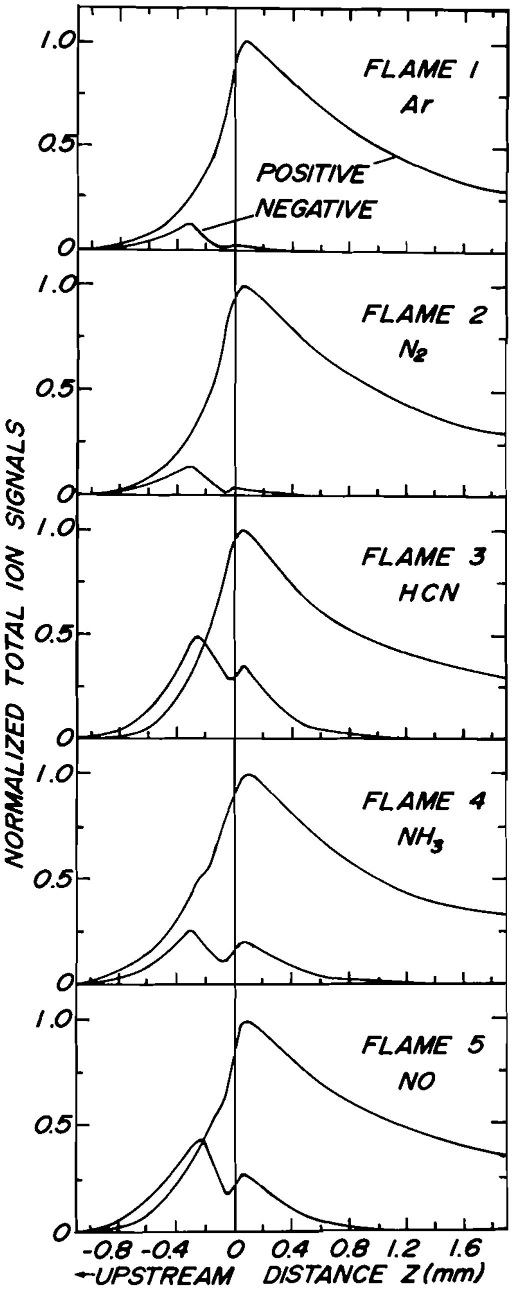

FIG. 1. Positive and negative total ionization profiles for flames 1–5 with added Ar, N_2, HCN, NH_3, and NO, respectively. The curves are normalized to unity at the peaks of the positive ion profiles.

peak negative ion signal in the reaction zone is apparent for each of the fuel-N additives (HCN > NO > NH_3) compared with the signals observed for flames 1 (Ar) and 2 (N_2). In flames 1 and 2, the primary negative ion formation process is three-body electron attachment to oxygen (13)

[3] $e^- + O_2 + M \rightleftharpoons O_2^- + M \qquad \Delta G^0_{1800} = 16.8$

(Standard free energies and enthalpies of reaction are quoted in kJ mol^{-1} based on data from JANAF Tables (14). The subscript temperature of 1800 K is typical in these flames for a region near the middle of the reaction zone.) Secondary negative ions are formed rapidly in the reaction zone; e.g., by charge transfer from O_2^-. The negative ion spectrum for each of flames 3 and 4 is dominated by CN^- (given later in Fig. 3), arising from proton abstraction from HCN by a basic source ion

[4] $X^- + HCN \rightarrow CN^- + HX$

or possibly three-body attachment to CN radicals

[5] $e^- + CN + M \rightarrow CN^- + M \qquad \Delta H^0_{1800} = -406$

or, probably to a much smaller extent, dissociative electron attachment to HCN

[6] $e^- + HCN \rightarrow CN^- + H \qquad \Delta H^0_{1800} = 118$

which is quite endothermic. The high electron affinity of CN (EA = 3.8 eV) and moderate base strength of CN^- (proton affinity PA = 1468 kJ mol^{-1} at 1800 K) cause CN^- to be a comparatively stable species in the chemical environment of the reaction zone, resulting in the negative ion enhancement observed for flames 3 and 4. That the peak signal for flame 4 is lower is not surprising: the added NH_3 must first react to form HCN (or perhaps CN) before CN^- can be formed. The data indicate that roughly half of the NH_3 is converted to HCN at a point midway through the reaction zone.

On the other hand, the negative ion spectrum for flame 5 is dominated by approximately equal contributions from CN^- and NO_2^- (given later in Fig. 3). The large CN^- signal indicates a rapid chemical conversion of nearly half the NO additive to HCN halfway through the reaction zone. Presumably NO_2^- is formed by three-body electron attachment to NO_2, or by charge transfer to NO_2 from O_2^-. Evidently an appreciable amount of NO is oxidized to NO_2 in the reaction zone of this fuel-rich flame before the molecular oxygen is exhausted downstream. The important point demonstrated is the rapid conversion of NH_3 (flame 4) and NO (flame 5) to HCN; this is consistent with Morley's statement (4) that the chemical "route passes through HCN and this compound is formed quantitatively from fuel nitrogen irrespective of its chemical nature".

Finally, the observation that the total negative ion signal appears to exceed the positive ion signal upstream in flames 3 and 5 is, at first, surprising for a quasi-neutral flame plasma. The phenomenon was encountered previously for fuel-lean, CH_4–O_2 (13) and CH_3OH–O_2 (15) flames. An explanation was offered in terms of the back-diffusion of electrons a distance of the order of a Debye length followed by three-body attachment to electronegative O_2 molecules in the cooler unburnt gas upstream where the O_2 concentration is highest. The [negative ion]/[free electron] concentration ratio is shifted in favour of negative ions if an additive results in the formation of negative ions more stable than O_2^- in the flame environment. As described above, these are CN^- in flame 3, NO_2^- and CN^- in flame 5 and, to a lesser extent, CN^- in flame 4.

Individual Ion Profiles

Nearly all profiles observed for nitrogenous ion species, both positive and negative (and many non-nitrogenous ones also), exhibit the same basic double-peaked structure illustrated in Fig. 2 at +16 amu ($\sim NH_2^+$) for flame 4 with added NH_3; the ratio of the upstream/downstream peak magnitudes can vary considerably, however. The reasons for this profile structure encountered in fuel-rich flames have been discussed previously (1, 7, 13). Although the reaction zone is only about 0.3 mm thick extending back from $z = 0$, it appears thicker in profiles such as Fig. 2 because the distance scale is spread out upstream when a conical flame is sampled along its axis; even when the mass-spectrometer sampling probe is inserted well upstream of $z = 0$, ions can still diffuse through the orifice from the inside surface of the truncated luminous cone.

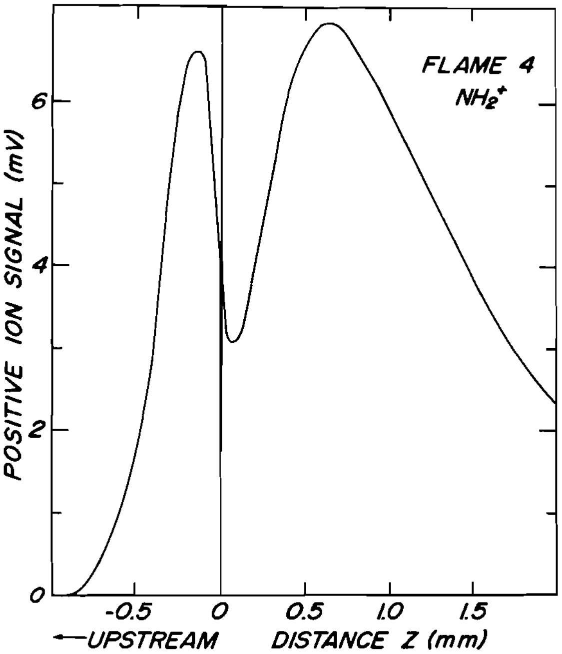

FIG. 2. Typical double-peaked profile structure observed for most individual ionic species, both positive and negative. The curve shown was recorded at +14 amu in flame 4 with the NH_3 additive. The reaction zone is located upstream of $z = 0$.

We shall confine our attention here to the profile peaks occurring upstream in the reaction zone. The presentation of profiles at all relevant mass numbers (m/e) would constitute an overwhelming body of data. Instead, we shall characterize the upstream peaks in terms of two simple parameters: the peak height, and the peak position on the distance scale z. The peak heights are presented in Fig. 3 for each mass number as a "histogram" giving the peak magnitudes of the ion signals for flames 1–5 (with added Ar, N_2, HCN, NH_3, and NO, in order). Similarly, a peak position plot is given in Fig. 4 where the horizontal lines indicate an uncertainty in peak position of ±0.02 mm; the uncertainty can be larger for small, broad peaks, however. In both Figs. 3 and 4, selected ionic species are placed into one of six groups depending upon the role played by the species.

In general, the nitrogenous ions in the reaction zone are formed by chemical ionization (CI) processes involving a source ion reacting with a nitrogenous neutral. The first group in Fig. 3, labelled positive source ions, consists of the major protonated species in the reaction zone which can

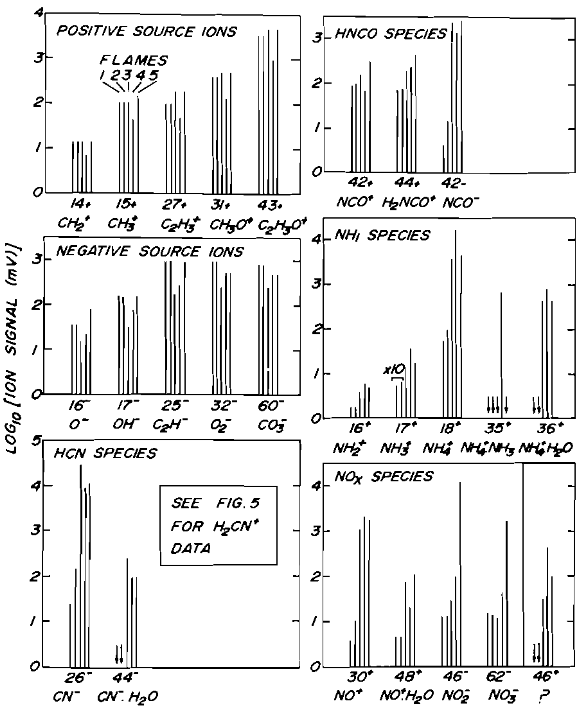

FIG. 3. Histograms for individual mass numbers m/e giving the profile magnitudes of the upstream peaks occurring in the reaction zone. Each histogram consisting of five vertical lines, from left to right, represents the peak heights measured in flames 1–5 with added Ar, N_2, HCN, NH_3, and NO, respectively.

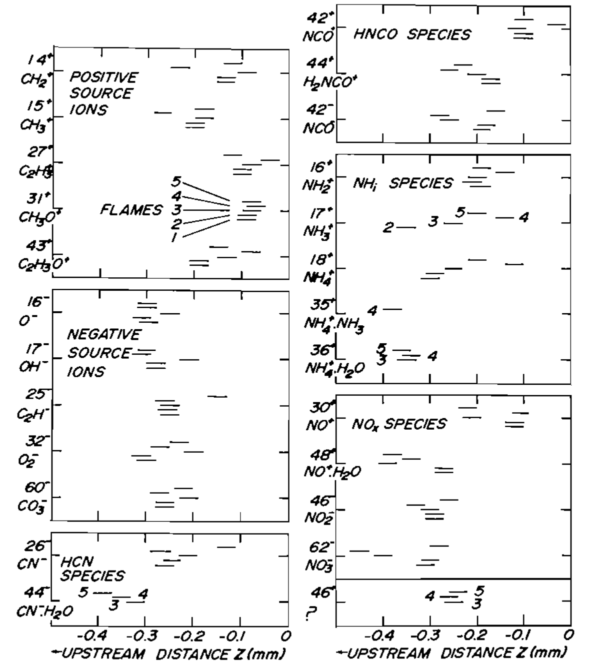

FIG. 4. Profile peak position plot for individual mass numbers *m/e* giving the peak positions on the flame axis of the upstream peaks occurring in the reaction zone. Each group of five horizontal lines, from bottom to top, represents the peak positions measured with an uncertainty of ±0.02 mm in flames 1–5 with added Ar, N_2, HCN, NH_3, and NO, respectively.

chemically ionize neutrals by proton transfer. The striking similarity of the histograms is evident. The very high proton affinity of ammonia causes all five source ions to be depleted in flame 4. The histograms of the second group, labelled negative source ions, again show a basic similarity to each other. All five source ions are depleted by proton transfer reactions with HCN to form CN^- in flames 3 and 4; flame 4 requires the prior conversion of NH_3 to HCN as mentioned above in the discussion of total ion profiles. The least regular behaviour is evident for the NO addition in flame 5. The net reaction of OH^- and C_2H^- is very small. The reaction

[7] $O_2^- + NO \rightarrow O^- + NO_2$

could account for the decrease of O_2^- and increase of O^-. The CO_3^- peak will be depleted by the known reaction (16)

[8] $CO_3^- + NO \rightarrow NO_2^- + CO_2$

With regard to the peak position plot given in Fig. 4, the actual peak position of a given ion signal is a less meaningful parameter than the peak magnitude. Downstream in the burnt gas, the peak positions provide some evidence for a chemical sequence of the nitrogenous species N_2–HCN/CN–HNCO/NCO–NH_i (i = 0–3)–NO_x (1, 4). No such sequence is evident in the spatially-limited reaction zone. In fact, the peak position of a nitrogenous ion is more revealing of its source ion than the nitrogenous neutral from which it is made. This situation can sometimes be used to advantage to clarify the dominant CI process. Figure 4 is also useful for the identification of cluster ions which tend to peak far upstream at lower temperature.

In addition to the positive and negative source ions given in Figs. 3 and 4, the remaining four groups of ions provide evidence for particular nitrogenous neutrals in the reaction zone of the flame doped with various additives. These four groups designated as HCN species, HNCO species, NH_i species, and NO_x species will be discussed in turn.

HCN Species

Evidence for HCN and /or CN radicals is obtained from ion signals corresponding to CN^- and its hydrate $CN^-.H_2O$, and also from the H_2CN^+ profiles given in Fig. 5. The CN^- ions can be formed by proton transfer from HCN; e.g.

[9] $C_2H^- + HCN \rightleftharpoons CN^- + C_2H_2$

or by charge transfer to CN radicals from negative ions such as O^-, OH^-, C_2H^-, and O_2^-. This am-

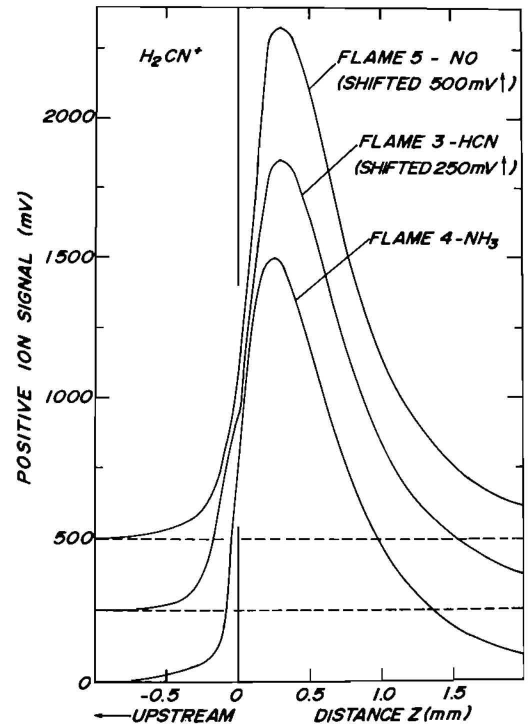

FIG. 5. Single-peaked profiles for H_2CN^+ at +28 amu in flames 3–5 with added HCN, NH_3, and NO, respectively. The peaks are displaced vertically to avoid overlapping.

biguity concerning the identity of the dominant source, neutral stable molecule or free radical, has occurred frequently in these studies (1). In an attempt to resolve the dilemma, consider the behaviour of flame 3 with 0.3% HCN additive. The HCN molecules will be attacked to form CN radicals by reactions such as (17, 18)

$$[10] \quad HCN + H \rightleftharpoons CN + H_2 \qquad \Delta G^\circ_{1800} = 58.6$$

or its OH/H_2O counterpart. In these fuel-rich flames, however, reaction [10] will tend to dominate. Assuming a forward rate constant k_{10} of 10^{-10} cm^3 $molecule^{-1}$ s^{-1}, reaction [10] has a relaxation time $\tau \simeq 1/k_{10}[HCN] = 0.1$ μs in the forward direction and considerably smaller in the reverse direction. The forward relaxation time corresponds to 5×10^{-5} mm on the flame axis, assuming a velocity midway in the reaction zone of 500 mm s^{-1} (downstream velocity $\simeq$ 1 m s^{-1}), so that reaction [10] will be locally balanced. Using mole fractions for H of 0.009 and H_2 of 0.25 obtained by Hastie (19) in the middle of the reaction zone of a very similar CH_4–O_2 flame and an equilibrium constant $K = 0.02$ at 1800 K, the equilibrium ratio $[CN]/[HCN] = K_{1800}[H]/[H_2] = 7 \times 10^{-4}$. Even if [CN] were to overshoot its local equilibrium value considerably, CN will still be a minor species compared with HCN. Thus, the formation of CN^- by proton transfer from HCN should dominate its formation by charge transfer to CN radicals. Even for the flames 2, 4, and 5 involving nitrogenous additives other than HCN, the same considerations should apply. Therefore, the high CN^- peak magnitudes in Fig. 3 for flames 4 and 5, only slightly less than that for flame 3, illustrate the rapid conversion of NH_3 and NO to HCN.

If a reaction such as [10] is locally balanced in the reaction zone, the same should be true for the proton transfer reactions like [9] or

$$[11] \quad OH^- + HCN \rightleftharpoons CN^- + H_2O$$

since their relaxation times involve ion–molecule rate constants which are even larger than k_{10}. Not surprisingly, the CN^- peak shapes follow those of the major negative source ions as indicated in Fig. 4; the corresponding peak positions of CN^- and C_2H^- are remarkably similar.

The relative magnitudes of the $CN^-.H_2O$ peaks in Fig. 3 are very nearly 1% of the corresponding CN^- peaks in flames 3, 4, and 5. The signals at −44 amu are assigned to the CN^- hydrate on the basis of the peak position plot in Fig. 4; the hydrate signals peak considerably upstream of CN^- where the lower flame temperature favours hydrate formation.

The H_2CN^+ profiles are shown separately in Fig. 5 for flames 3, 4, and 5 since they represent one of the few cases where single-peaked profiles were observed. Nevertheless, the upstream tails through the reaction zone are considerable. The large positive source ions in the reaction zone involve species with proton affinities (PA's) > PA(HCN). The formation of appreciable H_2CN^+ must await the rise of H_3O^+ since PA(HCN) > PA(H_2O) (20). Once again, a rough calculation of the relaxation times for the forward and reverse directions of

$$[12] \quad H_3O^+ + HCN \rightleftharpoons H_2CN^+ + H_2O$$

indicates that reaction [12] is locally balanced. Thus, the shapes of the H_2CN^+ profiles are dominated by the corresponding H_3O^+ profiles in the reaction zone and for some distance downstream. The slight upstream shoulder apparent for the HCN additive profile in Fig. 5 is explicable in terms of the production of H_2CN^+ via an exothermic proton transfer reaction such as

$$[13] \quad C_2H_3^+ + HCN \rightleftharpoons H_2CN^+ + C_2H_2$$

where PA(HCN) > PA(C_2H_2) at room temperature (20, 21).

It should also be mentioned that the profiles at +45 amu for flames 1–5 (not presented in the figures) showed the usual double-peaked structure except that flame 4 with the NH_3 additive had a third peak relatively far upstream at $z = -0.30$ mm indicative of $NH_4^+.HCN$ cluster ions. As a final observation concerning the HCN species, no clear evidence was obtained for either CN^+ or HCN^+. This is not surprising in view of the fact that the CN radical has a high ionization energy and a low proton affinity.

In summary, these ion data show the rapid conversion of NH_3 and NO to HCN. At a given point z in the reaction zone, the signal magnitudes for each of CN^-, $CN^-.H_2O$, and H_2CN^+ invariably exhibit the order flame 3 (HCN) > flame 5 (NO) > flame 4 (NH_3) for 0.3% of these three fuel-N additives. The results suggest the existence of a direct chemical path linking HCN and NO involving CH_i radicals

$$[14a] \quad CH_i(i = 1\text{–}3) + NO \rightleftharpoons HCN + H_{i-1}O(i = 1\text{–}3)$$

$$[14b] \qquad \rightleftharpoons CN + H_iO(i = 1, 2)$$

All five reactions [14] are exothermic in the forward direction.

HNCO Species

The large NCO^- signals observed at −42 amu in flames 3, 4, and 5 may be formed by proton transfer from HNCO or charge transfer to NCO radicals. Several authors have postulated the oxidation of HCN/CN to form HNCO/NCO (4, 22–24) although direct evidence of the latter species is lacking. Pre-

TABLE 1. Structural features of profiles at −42 amu in the reaction zone

		Upstream		Downstream	
Flame	Additive	z(mm)	Feature	z(mm)	Feature
2	N_2	−0.32	Slight shoulder	−0.18	Main peak
3	HCN	−0.26	Main peak	−0.10	Second peak, barely resolved
4	NH_3	−0.28	Single peak		
5	NO	−0.25	Slight shoulder	−0.16	Main peak

sumably the species are linked by fast balanced reactions

[15*a*] $HNCO + H \rightleftharpoons NCO + H_2 \qquad \Delta G^0_{1800} = 25.2$

[15*b*] $HNCO + OH \rightleftharpoons NCO + H_2O \qquad \Delta G^0_{1800} = -15.8$

Using Hastie's concentration values (19) and data from JANAF Tables (14), the equilibrium ratio [NCO]/[HNCO] = 7×10^{-3} at 1800 K. Although this ratio is an order of magnitude larger than [CN]/[HCN], a similar conclusion seems justified. That is, NCO is a relatively minor species compared with HNCO, so that the formation of NCO^- by proton transfer from HNCO will dominate its formation by charge transfer to NCO radicals in the reaction zone.

Although the profiles at −42 amu have the usual double-peaked shape, the peak in the reaction zone of flames 2, 3, and 5 shows further structure in addition to the main peak position given in Fig. 4; these details are listed in Table 1. One possible interpretation involves the two isomeric forms HNCO/NCO (designated form A, having a CO bond) and HCNO/CNO (form B, with an NO bond). However, it is difficult to associate one particular isomeric form with the upstream or downstream position of the features. Perhaps the rising concentration of CO favours form A in the downstream position. In any case, the similar magnitude of the major peaks in flames 3, 4, and 5 again illustrates the rapid interconversion of the fuel-N additives in the reaction zone.

The histogram at +42 amu in Fig. 3 is similar to those designated as positive source ions with one difference; the enhanced peak height for flame 5 provides possible evidence for ionized NCO radicals. Also, the enhanced signals in flames 3–5 at +44 amu provide reasonably good evidence for protonated HNCO. The peak heights are not consistent with an assignment as $^{13}C^{12}CH_3O^+$ stemming from the large source ion signals at +43 amu representing protonated ketene. Nor is N_2O^+ a likely contender in view of the high ionization energy of $N_2O \sim 13$ eV; the preferred source reaction involving charge transfer from O^+ (1, 25) is highly unlikely in a fuel-rich flame where O^+ was not detected.

NH_i Species

The histograms in Fig. 3 at +16, 17, and 18 amu are distinctly different from those at +14 and 15 amu. Major contributions to the former arise from protonated NH_i (i = 1–3) species whereas the latter represent CH_2^+ and CH_3^+, respectively. No evidence was obtained for NH^+ at +15 amu. From Fig. 4, the peak positions of the NH_i^+ ions in flames 3–5 are similar. If the NH_i species are protonated by the same source ions, the evidence is indicative of a rapid interconversion of the NH_i species

[16] $NH_i + H(OH) \rightleftharpoons NH_{i-1} + H_2(H_2O)$

for i = 2, 3. Presumably the very high proton affinity of NH_3 leading to the very large NH_4^+ signal detected in flame 4 accounts for the depression of all of the positive source ions in flame 4 as shown in Fig. 3. In conclusion, it is again worth emphasizing the evidence presented by this data for the rapid interconversion of the fuel-N additives; in this case, the conversion of HCN and NO to NH_3, NH_2, and NH.

Of minor interest are a number of cluster ions assigned on the basis of their peak positions shown relatively far upstream in Fig. 4. These include $NH_4^+.NH_3$ at +35 amu which was observed only in flame 4 with the NH_3 additive, and $NH_4^+.H_2O$ at +36 amu for flames 3–5.

NO_x Species

From Fig. 3, the NO^+ signals at +30 amu in flames 3–5 are of comparable magnitude. At first glance it is somewhat surprising to find the largest signal in flame 4 with the NH_3 additive. The probable explanation offers some confirmation of a mechanism discussed previously (1), involving a contribution from $CH_2NH_2^+$, also at +30 amu, by condensation reactions of $NH_i^+ + CH_j$ or $CH_j^+ + NH_i$ (26). This explanation is reinforced by the peak position in Fig. 4, since the signals at +30 amu in flames 3 and 5 peak upstream of the flame 4 peak; the latter occurs in close proximity to those of the NH_i^+ ions. Presumably the major portion of the signals in flames 3 and 5 is due to NO^+ produced by exothermic charge transfer to NO by source ions such as CH_3^+ and CH_2^+. Similar *relative* peak positions at +48 amu occurring considerably further upstream are indicative of hydrate ions. However, the depressed peak height for flame 4 shown in Fig. 3 is consistent with $CH_2NH_2^+.H_2O$ being less stable than $NO^+.H_2O$.

The NO_2^- ions at −46 amu can be produced by exothermic charge transfer to NO_2 by O^-, OH^-, and O_2^-. However, NO_2 is not expected to be abundant in these fuel-rich flames. A probable major formation mechanism involving NO directly, particularly in flame 5, is

[8] $CO_3^- + NO \rightarrow NO_2^- + CO_2$

as discussed previously (1). Certainly the signals at −46 amu peak together in a group in proximity to the CO_3^- peaks, as shown in Fig. 3. The peaks at −46 amu in flames 1 and 2 are due to isotopic $^{13}CHO_2^-$ from the very large $^{12}CHO_2^-$ signals detected at −45 amu. Data at −45 amu have not been included as source ions because the profiles are remarkably constant over the range of flames 1–5. Nevertheless, they provide a useful internal "calibration standard" for comparing other negative ion profile magnitudes in the various flames.

The signals observed at −62 amu cover a wide range on the peak position plot, Fig. 4. In these fuel-rich flames, it is probable that the signal represents NO_3^- only in flame 5, formed by the known reaction (16)

[17] $CO_3^- + NO_2 \rightarrow NO_3^- + CO_2$

The peak positions for flames 3 and 4 located very far upstream are indicative of hydrates, most probably $CN^-.2H_2O$; another possibility for flame 4 is $CHO_2^-.NH_3$ since an additional shoulder is observed on the profile at $z = -0.30$ mm.

Finally, the nitrogenous ions at +46 amu in flames 3–5 shown at the lower right of Figs. 3 and 4 present a problem of assignment; all of NO_2^+, $H_2CN^+.H_2O$, $NH_4^+.CO$, and CH_4NO^+ have the right mass number (m/e). However, the signal is largest for the NH_3 additive, and the peak positions given in Fig. 4 are not indicative of cluster ions. We believe the most logical candidate to be CH_4NO^+, interpreted as protonated formamide $NH_2CHO.H^+$. The parent molecule can be formed from the reaction of NH_3 with formaldehyde.

[18] $NH_3 + HCHO \rightarrow NH_2CHO + H_2$

and considerable formaldehyde is present in the reaction zone of these flames (detected as the source ion CH_3O^+).

Conclusions

These studies in the reaction zone of a fuel-rich hydrocarbon flame with fuel-N additives provide confirmation of many of the mass assignments and mechanisms discussed previously for N_2 addition (1). The nitrogenous chemistry, both neutral and ionic, is much easier to sort out using the fuel-N additives, however. The present results also indicate the presence of formamide, a new species not previously detected. When ions are used to probe the neutral chemistry, a question frequently arises: is a given nitrogenous ion representative of a related nitrogenous neutral (e.g., NO^+ from NO), formed in a simple chemical ionization process such as proton transfer or charge transfer? Or, is the identity obscured by a more complicated ion–molecule source reaction involving rearrangement or condensation (e.g., NO_2^- from NO, not NO_2; $CH_2NH_2^+$ as well as NO^+ at +30 amu)? The present experiments answer this question in a number of important cases.

The picture emerging from these studies is that of a spatially limited reaction zone containing a wide variety of nitrogenous neutral intermediates intermingled together, temporally independent of the nitrogen source. The main value of the additive approach is realized when one adds a neutral species (HCN, NH_3, NO) and observes a nitrogenous ion signal which cannot reasonably result from a direct ion–molecule reaction of the neutral flame ions. In this circumstance, rapid interconversion of the nitrogenous neutrals can be demonstrated, the ions merely functioning as a probe of the neutral chemistry.

Acknowledgements

Support of this work by the Natural Sciences and Engineering Research Council of Canada under Grant Numbers A1604 (J.M.G.) and A6258 (D.K.B.) is acknowledged.

1. G. B. De Brou, J. M. Goodings, and D. K. Bohme. Combust. Flame, **39**, 1 (1980).
2. C. P. Fenimore. Thirteenth Symposium (International) on Combustion. The Combustion Institute, Pittsburgh, PA. 1971. p. 373.
3. A. N. Hayhurst and I. M. Vince. Prog. Energy Combust. Sci. **6**, 35 (1980).
4. C. Morley. Combust. Flame, **27**, 189 (1976).
5. E. M. Bulewicz and P. J. Padley. Ninth Symposium (International) on Combustion. Academic Press, New York. 1963. p. 638.
6. Chun-Wai Ng. M.Sc. Thesis, York University, Downsview, Ont., Canada M3J 1P3. 1977.
7. J. M. Goodings, Chun-Wai Ng, and D. K. Bohme. Combust. Flame, **36**, 27 (1979).
8. H. F. Calcote. Eighth Symposium (International) on Combustion. Williams & Wilkins, Baltimore, MD. 1962. p. 184.
9. K. N. Bascombe, J. A. Green, and T. M. Sugden. Adv. Mass Spectrom. **2**, 66 (1962).
10. C. Bertrand and P. J. Van Tiggelen. J. Phys. Chem. **78**, 2320 (1974).
11. A. van Tiggelen, J. Peeters, and C. Vinckier. Thir-

teenth Symposium (International) on Combustion. The Combustion Institute, Pittsburgh, PA. 1971. p. 311.

12. B. L. CHAWNER and A. T. BLADES. Can. J. Chem. **56**, 2278 (1978).
13. J. M. GOODINGS, CHUN-WAI NG, and D. K. BOHME. Combust. Flame, **36**, 45 (1979).
14. JANAF Thermochemical Tables. (*a*) D. R. STULL, H. PROPHET *et al.* NSRDS-NBS 37, 2nd ed. U.S. Government Printing Office, Washington, DC. 1971; (*b*) M. W. CHASE, J. L. CURNUTT, A. T. HU, H. PROPHET, A. N. SYVERUD, and L. WALKER. 1974 Supplement, J. Phys. Chem. Ref. Data, **3**, 311 (1974); (*c*) M. W. CHASE, J. L. CURNUTT, H. PROPHET, R. A. McDONALD, and A. N. SYVERUD. 1975 Supplement, J. Phys. Chem. Ref. Data, **4**, 1 (1975).
15. J. M. GOODINGS, CHUN-WAI NG, and D. K. BOHME. Int. J. Mass Spectrom. Ion Phys. **29**, 57 (1979).
16. F. C. FEHSENFELD and E. E. FERGUSON. J. Chem. Phys. **61**, 3181 (1974).
17. P. M. RENZEPIS and T. M. SUGDEN. Nature, **202**, 448 (1964).
18. J. C. BODEN and B. A. THRUSH. Proc. R. Soc. London Ser. A, **305**, 107 (1968).
19. J. W. HASTIE. Combust. Flame, **21**, 187 (1973).
20. K. TANAKA, G. I. MACKAY, and D. K. BOHME. Can. J. Chem. **56**, 193 (1978).
21. W. A. CHUPKA, J. BERKOWITZ, and K. M. A. REFAEY. J. Chem. Phys. **50**, 1938 (1969).
22. B. HAYNES, D. IVERACH, and N. Y. KIROV. Fifteenth Symposium (International) on Combustion, The Combustion Institute, Pittsburgh, PA. 1975. p. 1103.
23. J. MULVIHILL and L. F. PHILLIPS. Fifteenth Symposium (International) on Combustion, The Combustion Institute, Pittsburgh, PA. 1975. p. 113.
24. C. P. FENIMORE. Combust. Flame, **26**, 249 (1976).
25. G. B. DE BROU. M.Sc. Thesis, York University, Downsview, Ont., Canada M3J 1P3. 1980.
26. D. SMITH and N. G. ADAMS. Chem. Phys. Lett. **47**, 145 (1977).